Journal of Molecular and Cellular Cardiology 120 (2018) 1–11

Contents lists available at ScienceDirect

Journal of Molecular and Cellular Cardiology

journal homepage: www.elsevier.com/locate/yjmcc

TRPV6 protects ER stress-induced apoptosis via ATF6α-TRPV6-JNK pathway in human embryonic stem cell-derived cardiomyocytes

Zhichao Li[a,b,e,1], Zhaoyue Meng[c,1], Jun Lu[a,b,e], Francis M. Chen[c], Wing-Tak Wong[c], Gary Tse[b,d,e], Changbo Zheng[a,b,e,f], Wendy Keung[g], Kennis Tse[g], Ronald A. Li[g,h], Liwen Jiang[c], Xiaoqiang Yao[a,b,e,*]

[a] School of Biomedical Sciences, The Chinese University of Hong Kong, Hong Kong, China
[b] Li Ka Shing Institute of Health Science, The Chinese University of Hong Kong, Hong Kong, China
[c] School of Life Sciences and State Key Laboratory of Agrobiotechnology, The Chinese University of Hong Kong, Hong Kong, China
[d] Department of Medicine and Therapeutics, The Chinese University of Hong Kong, Hong Kong, China
[e] Shenzhen Research Institute, The Chinese University of Hong Kong, Shenzhen, Hong Kong, China
[f] School of Pharmaceutical Science and Yunnan Key Laboratory of Pharmacology for Natural Products, Kunming Medical University, Kunming, Yunnan, China
[g] Dr. Li Dak-Sum Centre, The University of Hong Kong – Karolinska Institutet Collaboration in Regenerative Medicine, Hong Kong, China
[h] Ming-Wai Lau Centre for Reparative Medicine, Karolinska Institutet, Hong Kong, China

ARTICLE INFO

Keywords:
TRPV6 channel
Human embryonic stem cells
ER stress
ATF6
JNK signaling pathway

ABSTRACT

Human pluripotent stem cell-derived cardiomyocytes have potential applications in disease modeling and drug screening. Therefore, it is important to understand the mechanisms and signaling pathways underlying the survival and death of these cells. Endoplasmic reticulum (ER) stress is triggered by various cellular stresses that disturb protein folding in the ER. Cells cope with ER stress by activating the unfolded protein response (UPR), a homeostatic signaling network that orchestrates the recovery of ER function. In the present study, we hypothesized that ER stress may upregulate the expression of transient receptor potential channel TRPV6, which in turn serves to protect human embryonic stem cell-derived cardiomyocytes (hESC-CMs) from ER stress-induced apoptotic cell death. Indeed, we found that ER stress induced by thapsigargin and tunicamycin led to increased expression of TRPV6 via ATF6α signaling branch. siRNA-mediated knockdown of TRPV6 aggravated ER stress-induced apoptotic cell death, whereas overexpression of TRPV6 attenuated ER stress-induced apoptosis in hESC-CMs. Furthermore, the signaling pathway downstream of TRPV6 was MAPK-JNK. Taken together, these results provide strong evidence that, under ER stress, TRPV6 is upregulated to protect hESC-CMs from apoptotic cell death via ATF6α-TRPV6-JNK pathway.

1. Introduction

Secreted and membrane proteins are synthesized and folded in the endoplasmic reticulum (ER). Various pathophysiological stimuli, such as nutrient deprivation, hypoxia, inhibition of glycosylation, calcium depletion from the ER lumen, lead to accumulation and aggregation of unfolded and/or misfolded proteins in the ER and induce the unfolded protein response (UPR). In mammals, the UPR comprises three parallel signaling branches: inositol-requiring protein 1α (IRE1α)-X-box binding protein 1 (XBP1), PRKR-like ER kinase (PERK)-eukaryotic translation initiation factor 2α (eIF2α)-activating transcription factor 4 (ATF4), and activating transcription factor 6α (ATF6α) [1]. Initially, the UPR is a cytoprotective response promoting adaption to re-establish normal ER function, but excessive or prolonged UPR activates maladaptive arm of the UPR, resulting in cell apoptosis.

Human pluripotent stem cell-derived cardiomyocytes (hPSC-CMs) provide an unlimited source of human cardiomyocytes for potential applications in disease modeling, drug screening and cell-based heart therapies [2]. For disease modeling, PSC-CMs have been used as models to study ER stress-related cardiomyopathies such as cardiac hypertrophy [3,4] and ischemic/reperfusion injury [5,6]. Therefore, it is important to understand the mechanisms and signaling pathways underlying the survival and death of these stem cells, including ER stress response, the UPR and apoptotic cell death. Such basic knowledge should provide essential and valuable information for proper maintenance and disease modeling of hPSC-CMs. Up to the present, the

* Corresponding author at: School of Biomedical Sciences, The Chinese University of Hong Kong, Hong Kong, China.
E-mail address: yao2068@cuhk.edu.hk (X. Yao).
[1] these two authors contribute equally to the work.

https://doi.org/10.1016/j.yjmcc.2018.05.008
Received 1 December 2017; Received in revised form 27 April 2018; Accepted 10 May 2018
Available online 16 May 2018
0022-2828/

research regarding ER stress in cardiomyocytes is mostly based on animal experiments or primary cultured rodent cardiomyocytes. However, there are considerable differences in cardiac physiology between human and rodent cardiomyocytes [7]. By contrast, hPSC-CMs are suggested to have many properties of authentic cardiomyocytes [8,9]. Therefore, these cells may provide an ideal model system to study human heart diseases.

The transient receptor potential (TRP) channels are a superfamily of cation channels that have diverse physiological function. They can be grouped into six subfamilies: TRPC, TRPV, TRPM, TRPP, TRPML and TRPA [10]. Some TRP channels have been reported to be involved in ER stress and cell viability. For example, TRPC1 may inhibit the UPR and thus contribute to neuronal survival [11]. Conversely, TRPC3, TRPC6 and TRPV1 may increase ER stress, consequently promoting apoptotic death in endothelial cells, podocytes and lung epithelial cells [12–15].

TRPV6 is a highly Ca^{2+}-selective channel important for body Ca^{2+} homeostasis. TRPV6 knockout mice show various phenotypes linked to impaired Ca^{2+} homeostasis, such as impaired fertility, defective Ca^{2+} absorption, and lower body weight [16]. By contrast, upregulation of TRPV6 has been implicated in cancer progression [16,17]. TRPV6 is also an important regulator of cell apoptosis [17–20]. The activity of TRPV6 may either promote or inhibit cell apoptosis dependent on the cell types [17–20]. However, the role of TRPV6 in apoptotic cell death has never been studied in any stem cell model or in the context of ER stress response.

In this report, we hypothesized that, under ER stress, TRPV6 expression in hESC-CMs is upregulated as a part of UPR, and that the signaling pathway involves ATF6α-TRPV6. We further hypothesized that the upregulation of TRPV6 serves to protect hESC-CMs from ER stress-induced cell apoptosis. The results from this study demonstrated a cytoprotective role of TRPV6 in hESC-CMs under ER stress.

2. Materials and methods

2.1. ES cell culture and embryonic body differentiation

HES2 cell line was maintained in a feeder-free system in the mTeSR™1 medium on Matrigel (BD Biosciences)-coated plates. HES2 was differentiated into embryonic bodies (EBs) as described elsewhere [21]. Beating EBs were digested into single cardiomyocytes with collagenase type IV [21]. To purify cardiomyocytes, cells were infected with pLV-MLC2v-mGFP/mTdTomato-t2A-zeocin lentivirus particles, followed by zeocin selection [22].

2.2. Quantitative real-time PCR (qRT-PCR)

Total RNA was extracted from hESC-CMs using Trizol reagent (Invitrogen). cDNA was generated using SuperScript® First-Strand Synthesis System (Invitrogen). qRT-PCR was performed with 7500 Fast Real-time PCR system (Applied Biosystems, NY) using Power SYBR Green PCR Master Mix (Applied Biosystems, NY). The primer sequences were listed in Supplemental Table 1.

2.3. TUNEL assay

Apoptotic cardiomyocytes were detected using the terminal deoxynucleotidyl transferase-mediated dUTP nick-end labeling (TUNEL) method (Roche) as per the manufacturer's instructions.

2.4. Luciferase reporter constructs

The 5′-flanking sequence of human TRPV6 gene (GenBank™ accession number NM_018646.5) from nucleotides −573 to +31 was cloned into the pGL4.10 luciferase reporter vector (Promega). Truncated versions of human TRPV6 luciferase were also cloned into pGL4.10 luciferase reporter vector. Point mutation was performed using QuikChange II XL Site-Directed Mutagenesis Kit (Agilent Technologies, Santa Clara, CA).

2.5. Dual-luciferase reporter assay

hESC-CMs were co-transfected with the plasmids encoding the luciferase reporter constructs generated above together with internal control plasmid encoding Renilla luciferases. The cells were then infected with pAAV-sXBP1, or pAAV-ATF4, or pAAV-cleaved-ATF6α (1–373). 48 h after infection, the cells were washed with PBS and luciferases were measured.

2.6. Immunoblot analysis

hESC-CMs were lysed in RIPA buffer comprising 1% (vol/vol) Nonidet P-40, 150 mM NaCl, 20 mM Tris-HCl (pH 7.5), protease inhibitor cocktail (Roche) and phosphatase inhibitor cocktail (Roche). Protein concentrations were determined using the detergent-compatible protein assay (Bio-Rad, Hercules, CA). Boiled samples were subjected to SDS-PAGE and then transferred to polyvinylidene difluoride membranes. The following antibodies were used in immunoblot analysis: anti-ATF4 (1:1000, Proteintech Group),anti-ATF6 (1:1000, Abcam), anti-β-actin (1:2000, Santa Cruz), anti-Caspase-3 (1:1000, Cell Signaling Technology), anti-Caspase-12 (1:1000, Proteintech Group), anti-CHOP (1:1000, Proteintech Group), anti-GRP78 (1:1000, Proteintech Group), anti-HA (1:1000, TransGen Biotech), anti-phospho-SAPK/JNK Antibody (1:1000, Cell Signaling Technology), anti-SAPK/JNK Antibody (1:1000, Cell Signaling Technology), anti-TRPC5 (1:1000, Proteintech Group), anti-TRPM6 (1:1000, Alomone Labs), anti-TRPML1 (1:1000, Alomone Labs), anti-TRPP1 (1:500, Santa Cruz), anti-TRPV5 (1:1000, Alomone Labs), anti-TRPV6 (1:1000, Proteintech Group), anti-XBP1s (1:1000, Proteintech Group).

2.7. Lentiviral TRPV6-shRNA

Two short hairpin RNA (shRNA) constructs against human TRPV6 were generated using pLKO.1 puro vector containing a cassette for puromycin. The shRNA target sequences used were: TRPV6 sh1: GTA CATCATCTGCTTCACCAT, TRPV6 sh2: GGGAAACACAGTGTTACAC. Scrambled shRNA was used as the control. Lentiviral particles were produced in 293 T cells by co-transfecting pLKO.1 and packaging vectors. 48 h after transfection, the lentiviral supernatant was collected, centrifuged for 2 h at 50,000*g*, followed by re-suspension in cold PBS.

2.8. Adeno-associated virus (AAV)

The shuttle vectors used to generate pAAV-sXBP1, pAAV-ATF4 and pAAV-cleaved-ATF6α (1–373) were constructed by cloning respective cDNAs into the *Bam*HI and *Bgl*II sites in pAAV-MCS. AAV was packaged as described elsewhere [22]. In brief, the shuttle plasmids were co-transfected into HEK293T cells with pAAV-RC and pHelper plasmid. After transfection for 72 h, cells were harvested and viral particles were purified by PEG concentration.

2.9. ERAD assay

ER-associated degradation (ERAD) was performed using a TCR-α-HA plasmid as described elsewhere [23]. hESC-CMs were transfected with TCR-α-HA. 48 h later, the cells were treated with 360 μM cycloheximide (CHX) to inhibit protein synthesis, and harvested immediately or 30 min or 60 min following the addition of CHX. Immunoblot analysis was performed to determine the relative levels of TCR-α-HA/β-Actin.

2.10. Statistical analysis

All experiments were performed at least in triplicate. The results were expressed as mean ± SEM. Statistical significance was determined using Student's *t*-test, one-way analysis of variance (ANOVA) or two-way ANOVA using Prisms 6.0 software (GraphPad Software Inc., La Jolla, CA, USA). $P < 0.05$ was accepted as statistically significant.

Additional methods are provided in Online Supplemental Materials.

3. Results

3.1. Basic properties of differentiated hESC-CMs

EBs derived from human HES2 line showed spontaneous contractile activity as early as day 8 after induction of differentiation. Flow cytometry analysis performed on the differentiated HES2 cells at days 16–18 showed that 86% of cells were $cTnT^+$ [24]. Immunostaining experiments confirmed the expression of MLC2v, indicating that, after zeocin selection, almost all the cells were $MLC2v^+$ [24]. These $MLC2v^+$ cells displayed spontaneous beating with ~30 beats/min and had typical ventricular-like action potentials [21].

3.2. TG and TM upregulated the expression of ER stress markers in hESC-CMs

hESC-CMs were treated with two commonly used ER stress inducers, TG at 100 nM and TM at 2 μg/ml, for 6–24 h to induce ER stress. Both TG and TM increased the expression of two ER stress markers GRP78 and CHOP at mRNA and protein levels (Fig. S1A–E).

3.3. TG and TM increased the expression of TRPV6 in hESC-CMs

Quantitative RT-PCR was used to determine the mRNA levels of all TRP members in hESC-CMs (Fig. S2). Among all known TRP members, treatments with TG and TM for 24 h increased the mRNA levels of TRPC5, TRPM6, TRPML1, TRPP1, TRPV5 and TRPV6. Among them, TRPV6 mRNA had a greater increase of expression in response to TM and TG than other TRP members (Fig. S2). Time course experiments were performed for TRPV6. The results demonstrated that TG and TM treatments markedly increased the expression of TRPV6 at both mRNA (Fig. 1A-B) and protein levels (Fig. 1C-E) in a time-dependent manner. TG and TM treatments also increased the protein expression of TRPC5 and TRPV5, and to a less degree TRPML1 (Fig. S2E—F). Furthermore, TRPV6 expression was also detected in non-differentiated hESCs (Fig. S3).

3.4. Lack of effect for TRPV6 knockdown on the UPR in hESC-CMs

Two lentiviral-based TRPV6-shRNAs were constructed. As expected, knockdown of TRPV6 with two lenti-TRPV6-shRNAs decreased the expression of TRPV6 mRNA by ~75% and TRPV6 proteins by ~70% (Fig. 2A-C). However, knockdown of TRPV6 had no effect on the UPR, as indicated by expression level of two ER stress markers GRP78 and CHOP (Fig. 2D-F).

3.5. The ATF6 pathway of UPR regulated TRPV6 expression in hESC-CMs

As expected, ER stress inducers TG and TM stimulated all three branches of UPR signaling pathways, as indicated by increased expression of three transcription factors, i.e., sXBP-1, ATF4 and cleaved-ATF6α (Fig. 3A). To determine which branch is more relevant to TRPV6 upregulation, we co-expressed each individual transcription factor (carried by adeno-associated virus) with a TRPV6 promotor luciferase reporter plasmid in hESC-CMs. The results showed that, while all three transcription factors could stimulate TRPV6 expression, the cleaved-ATF6α had the strongest effect (Fig. 3B). qRT-PCR and immunoblot experiments further demonstrated that, while all three transcription factors could stimulate TRPV6 expression at mRNA level (Fig. 3C), only cleaved-ATF6α caused a statistically significant increase of TRPV6 proteins (Fig. 3D and E). These results suggest that the ATF6α signaling pathway is the main branch of UPR that could stimulate TRPV6 expression in hESC-CMs under ER stress. To verify these findings, we made deletion mutations at the putative ATF6 binding site of TRPV6 promoter (−246 to −241), followed by promotor luciferase reporter assay. As shown in Fig. 3A-B, the truncation mutant human-TRPV6 (−395/+31)-Luc, which did not interfere the putative ATF6 binding site, had little effect on TRPV6 expression. However, another truncation mutant human-TRPV6 (221/+31)-Luc, which removed the putative cleaved-ATF6α binding site, resulted in a significant decrease in TRPV6 expression (Fig. 4B). Moreover, a point mutation was introduced at the putative ATF6 binding site by substituting two nucleotides to generate a new construct M1 (Fig. 4C). Compared with human-TRPV6 (−573/+31)-Luc (WT), M1 resulted in a significant reduction of TRPV6 expression in luciferase reporter assay (Fig. 4D).

3.6. Knockdown of TRPV6 increased ER stress-induced apoptosis in hESC-CMs

We evaluated the effects of TRPV6 knockdown on ER stress-induced apoptosis of hESC-CMs using TUNEL and caspase assays. In TUNEL assay, compared to the control (lenti-scrambled shRNA), two lenti-TRPV6-shRNAs (si1 and si2) increased the percentage of TUNEL-positive apoptotic cells under ER stress (100 nM TG or 2 μg/ml TM for 48 h) (Fig. 5A-B). Caspase 12 is known to be involved in ER stress-induced apoptosis [25], whereas caspase-3 is the downstream executioner caspase leading to cell apoptosis [26]. As expected, TG and TM treatments both increased the level of cleaved caspase 12 (37 kD) (Fig. 5C and D) and cleaved caspase 3 (17 kD) (Fig. S4). Importantly, two lenti-TRPV6-shRNAs (si1 and si2) further enhanced the level of cleaved caspase 12 (Fig. 5C and D) and cleaved caspase 3 (Fig. S4) under ER stress. Together, these data suggest that TRPV6 protects against apoptotic cell death under ER stress in hESC-CMs.

3.7. Overexpression of TRPV6 reduced ER stress-induced apoptosis

To further confirm the protective role of TRPV6 against ER stress-induced apoptosis of hESC-CMs, we infected hESC-CMs with lentivirus carrying either TRPV6 (pLVX-TRPV6) or empty vector (pLVX-C) as control. As expected, lenti-pLVX-TRPV6 infection increased TRPV6 expression (Fig. 6A-B). Importantly, TRPV6 overexpression reduced the percentage of TUNEL-positive apoptotic cells under ER stress (Fig. 6C) and also reduced the level of cleaved caspase 12 under ER stress (Fig. 6D-E).

3.8. JNK signaling pathway was downstream of TRPV6

ER stress can stimulate JNK to activate apoptotic pathway [27]. Thus, we explored the possible relationship of MAPK-JNK with TRPV6. As expected, treatment of hESC-CMs with 100 nM TG or 2 μg/ml TM for 48 h resulted in JNK activation (Fig. 7A). Compared to the control with lenti-scrambled-shRNA, knockdown of TRPV6 with lenti-TRPV6-shRNAs (si1 and si2) further increased the JNK activity under ER stress, as indicated by increased level of p-JNK (Fig. 7A-B). Conversely, TRPV6 overexpression reduced the JNK activation under ER stress (Fig. 7C-D).

A JNK inhibitor SP600125 was used. Treatment with 20 μM SP600125 for 24 h markedly inhibited the activation of JNK (Fig. 7E-F). Interestingly, in the presence of 20 μM SP600125, lenti-TRPV6-shRNAs could no longer stimulate the JNK activity under ER stress (Fig. 7E-F). In addition, in the presence of SP600125, two lenti-TRPV6-shRNAs (si1 and si2) could no longer increase the percentage of TUNEL-positive apoptotic cells under ER stress (Fig. 7G). Collectively, these results suggest that TRPV6 acted through MAPK-JNK signaling pathway to

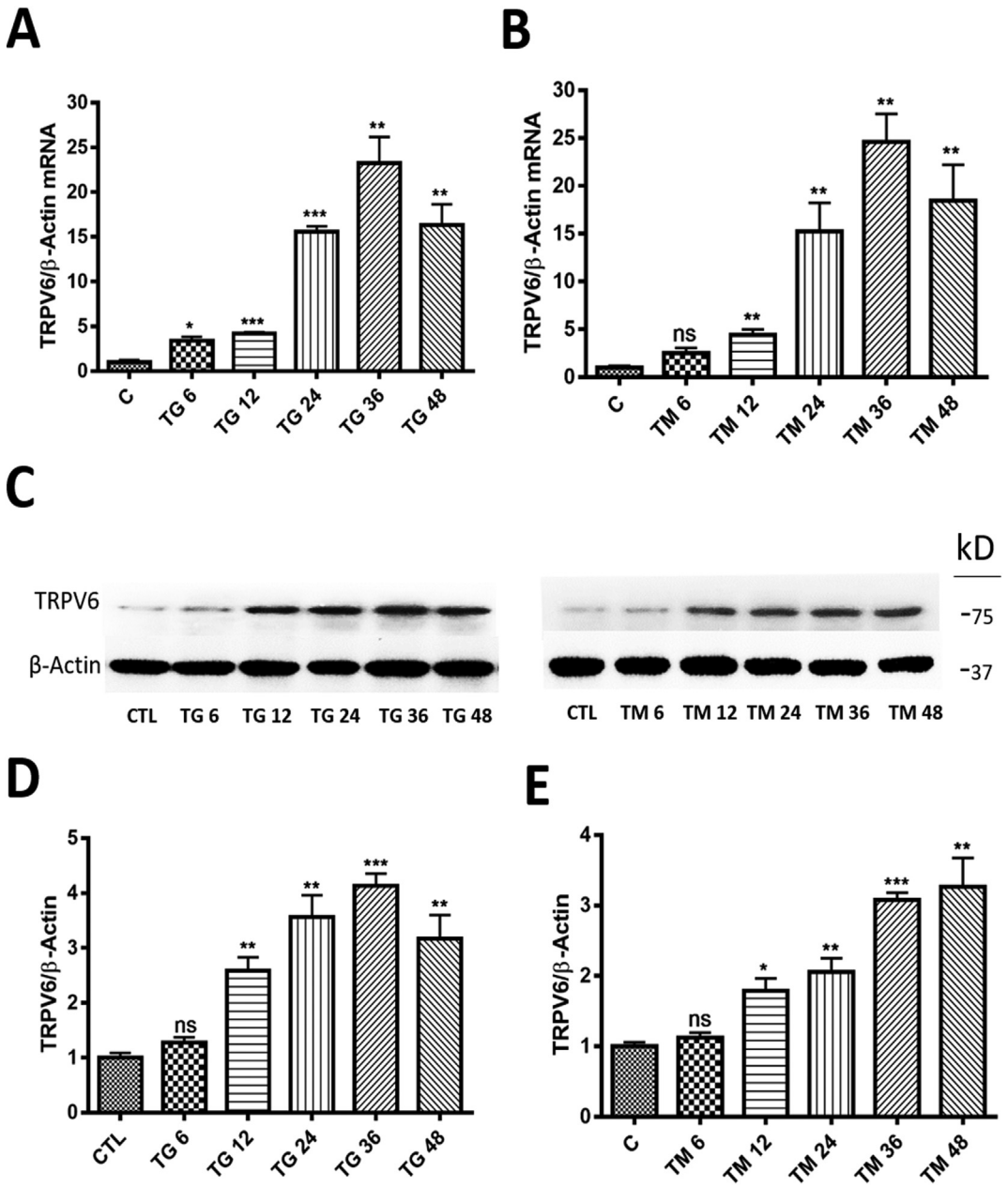

Fig. 1. ER stress increased the expression of TRPV6 in hESC-CMs. hESC-CMs were treated with TG (100 nM) or TM (2 μg/ml) for indicated 6–48 h. CTL stands for vehicle control without TG or TM treatment. A and B, relative mRNA expression of TRPV6 by qRT-PCR. C-E, protein level of TRPV6 by immunoblot. Mean ± SEM ($n = 3$ independent experiments). $^{*}P < .05$, $^{**}P < .01$, $^{***}P < .001$, ns = not significant.

exert its cytoprotective action against ER stress-induced apoptosis.

3.9. Knockdown of TRPV6 had no effect on ERAD

ERAD is an essential component of the adaptive ER stress response that serves to protect cardiomyocytes from ER stress-induced cell death [28]. We thus examined the relationship of TRPV6 with ERAD. Here, hESC-CMs were transfected with HA-tagged T-cell antigen receptor α-chain (TCR-α-HA) as an ERAD substrate, and the degradation of TCR-α-HA was determined by cycloheximide chase assay. However, we found that knockdown of TRPV6 with lenti-TRPV6-shRNAs had no effect on the degradation of TCR-α-HA (Fig. S5), suggesting that TRPV6 was not involved in ERAD.

3.10. Knockdown of TRPV6 did not alter spontaneous Ca^{2+} oscillations, while an ER stress inducer TG abolished the Ca^{2+} oscillations

We examined whether knockdown of TRPV6 could affect spontaneous Ca^{2+} oscillations in hESC-CMs. The cells were bathed in normal Ca^{2+}-containing physiological saline at 37 °C. Application of a β-adrenergic agonist isoprenaline at 10 μM increased the frequency of cytosolic Ca^{2+} oscillations. However, knockdown of TRPV6 with lenti-TRPV6-shRNA (si2) did not alter the frequency (Fig. S6A,B) and amplitude (Fig. S6A,C) of spontaneous and isoprenaline-stimulated cytosolic Ca^{2+} oscillations. Furthermore, overexpression of TRPV6 with lenti-pLVX-TRPV6 also had no effect on the spontaneous and isoprenaline-stimulated cytosolic Ca^{2+} oscillations (Fig. S6E,F,G).

However, treatment of cells with 100 nM TG, an ER stress inducer that depletes SR Ca^{2+} content, abolished the spontaneous and isoprenaline-stimulated cytosolic Ca^{2+} oscillations (Fig. S6D), which

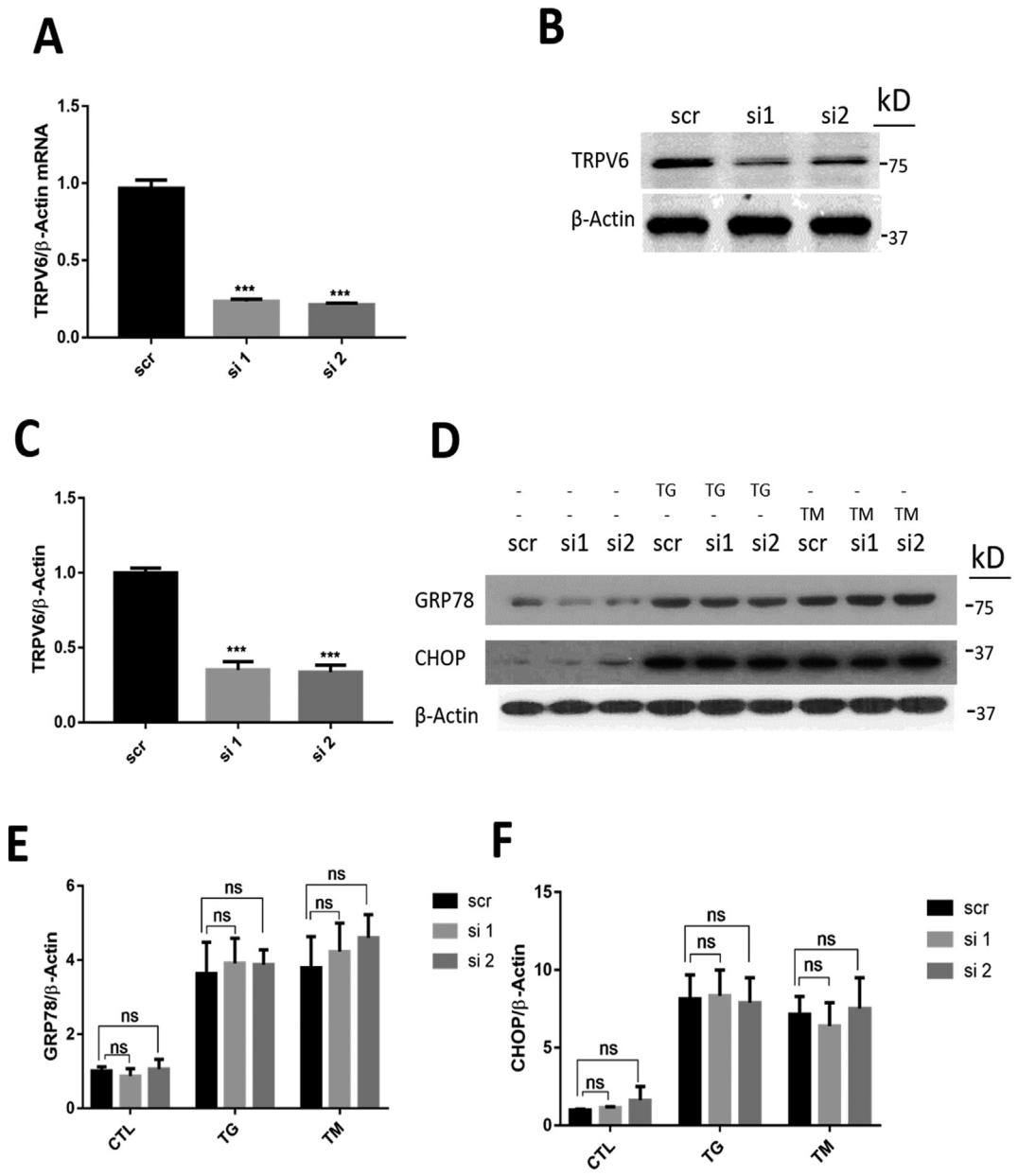

Fig. 2. Lack of effect for TRPV6 knockdown on the UPR. hESC-CMs were treated with lentivirus-based scrambled shRNA (scr), TRPV6-shRNA1 (si 1), or TRPV6-shRNA2 (si 2) for 72 h. A, relative mRNA expression of TRPV6 by qRT-PCR. B and C, representative images (B) and summary data showing the protein level of TRPV6. D-F, hESC-CMs were transfected with lentivirus-based shRNAs. These cells were further treated with vehicle (CTL), TG (100 nM), or TM (2 μg/ml) for 48 h, followed by immunoblot analysis of GRP78 and CHOP protein levels. Shown are representative images (D) and summary data (E and F). Mean ± SEM ($n = 3$ independent experiments). ***$P < .001$, ns = not significant.

could not be restored by knockdown or overexpression of TRPV6 (Fig. S6D,H).

3.11. Upregulation of TRPV6 expression in ischemia-reperfusion-treated hESC-CMs and in ischemia-injured heart

We next determined the effect of physiological stress of ischemia-reperfusion on TRPV6 expression in hESC-CMs. The results showed that ischemia-reperfusion increased the expression of TRPV6 proteins in hESC-CMs in immunoblots (Fig. S7A,B). Immunofluorescence staining further demonstrated an increased TRPV6 expression in individual hESC-CMs after TG or ischemia-reperfusion (Fig. S7C). As a confirmation, ischemia-reperfusion indeed induced ER stress as shown by an induction of truncated ATF6 (Fig. S7A,B).

A mouse model of myocardial infarction was established using left anterior descending artery ligation. Immunoblots showed that ischemic injury via left anterior descending artery ligation increased the expression of TRPV6 proteins in myocardial infarction heart (Fig. S7D,E). Immunostaining on thin tissue sections further confirmed an increased TRPV6 expression in ischemic injured heart tissue compared to sham-operated control (Fig. S7F.G). As a confirmation, artery ligation-induced ischemia indeed induced ER stress as shown by an induction of truncated ATF6 (Fig. S7D,E).

4. Discussion

In the present study, we explored the role of TRPV6 in the ER stress response in hESC-CMs and had the following major findings. 1) ER stress induction by TG, TM and ischemia-reperfusion caused a marked increase in the expressional level of TRPV6 proteins in hESC-CMs.

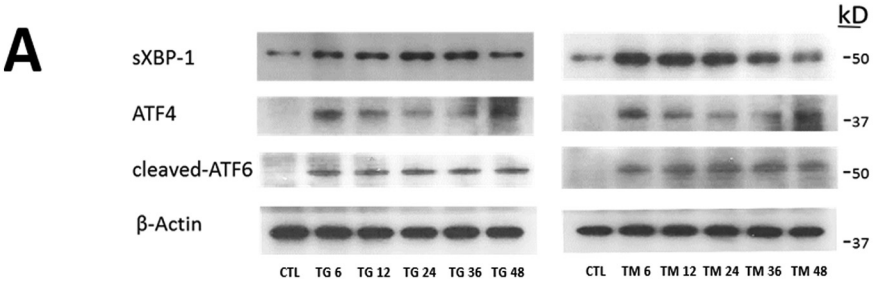

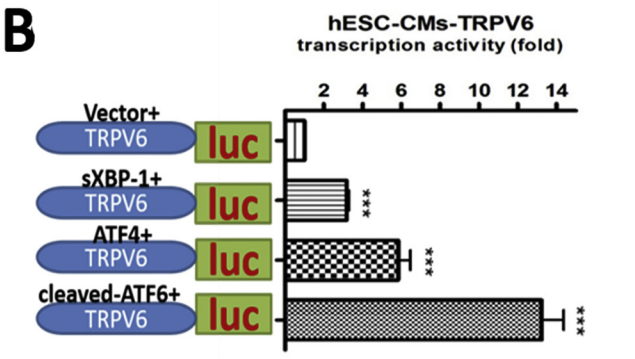

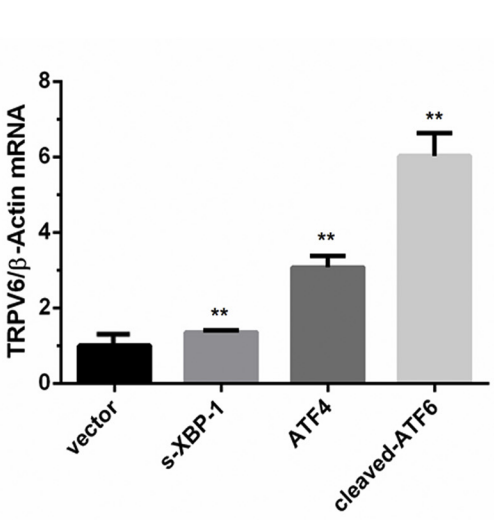

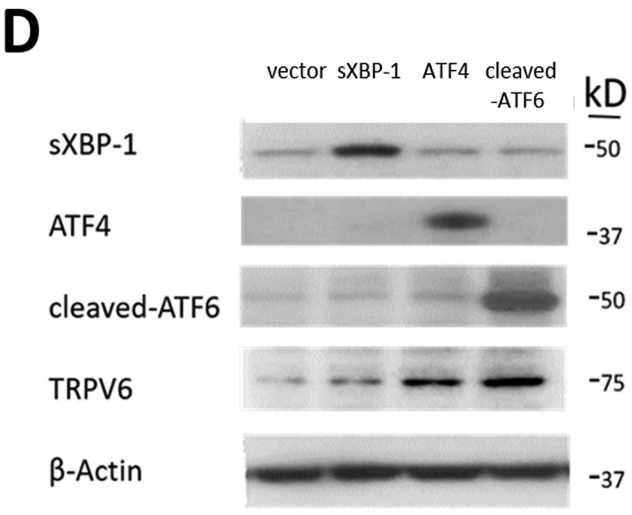

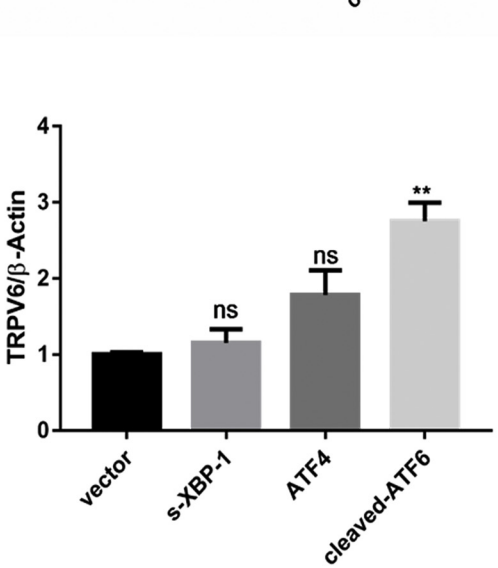

Fig. 3. The ATF6 pathway of the UPR caused TRPV6 up-regulation in hESC-CMs. A, hESC-CMs were treated with TG (100 nM) or TM (2 μg/ml) for 6–48 h, followed by immunoblot analysis of protein levels of sXBP-1, ATF4 and cleaved-ATF6α. CTL stands for vehicle control without TG or TM treatment. B, 5′-flanking sequence of human TRPV6 (−573/+31) containing TRPV6 promoter was cloned to luciferase reporter plasmid to generate human-TRPV6 (−573/+31)-Luc, followed by transfection to hESC-CMs. The cells were also infected with AAV-vector, AAV-sXBP-1, AAV-ATF4, or AAV-cleaved-ATF6α, respectively. Luciferase activity in each group was normalized to that in AAV-vector infected group. C, mRNA level of TRPV6 induced by AAV-sXBP-1, AAV-ATF4, or AAV-cleaved-ATF6α by qRT-PCR. D and E, representative immunoblot images (D) and summary data (E) showing protein level of TRPV6 induced by AAV-sXBP-1, AAV-ATF4, or AAV-cleaved-ATF6α. Mean ± SEM ($n = 3$ independent experiments). $^{**}P < .01$, ns = not significant.

TRPV6 expression was also upregulated in neonatal mouse heart in vivo after myocardial infarction. 2) Cleaved-ATF6 stimulated the TRPV6 expression in hESC-CMs. On the other hand, mutations at a putative ATF6 binding site in the promoter region of TRPV6 substantially reduced the ER stress-induced TRPV6 upregulation. 3) shRNA-mediated TRPV6 knockdown substantially increased the apoptotic cell death of hESC-CMs. Conversely, TRPV6 overexpression attenuated the apoptotic cell death. Taken together, these results provide strong evidence for the cytoprotective role of endogenous TRPV6 against ER stress-induced apoptosis in hESC-CMs.

Previously, several TRP isoforms, including TRPC1, −C3, −C6 and −V1, have been found to be associated with the UPR in various cell

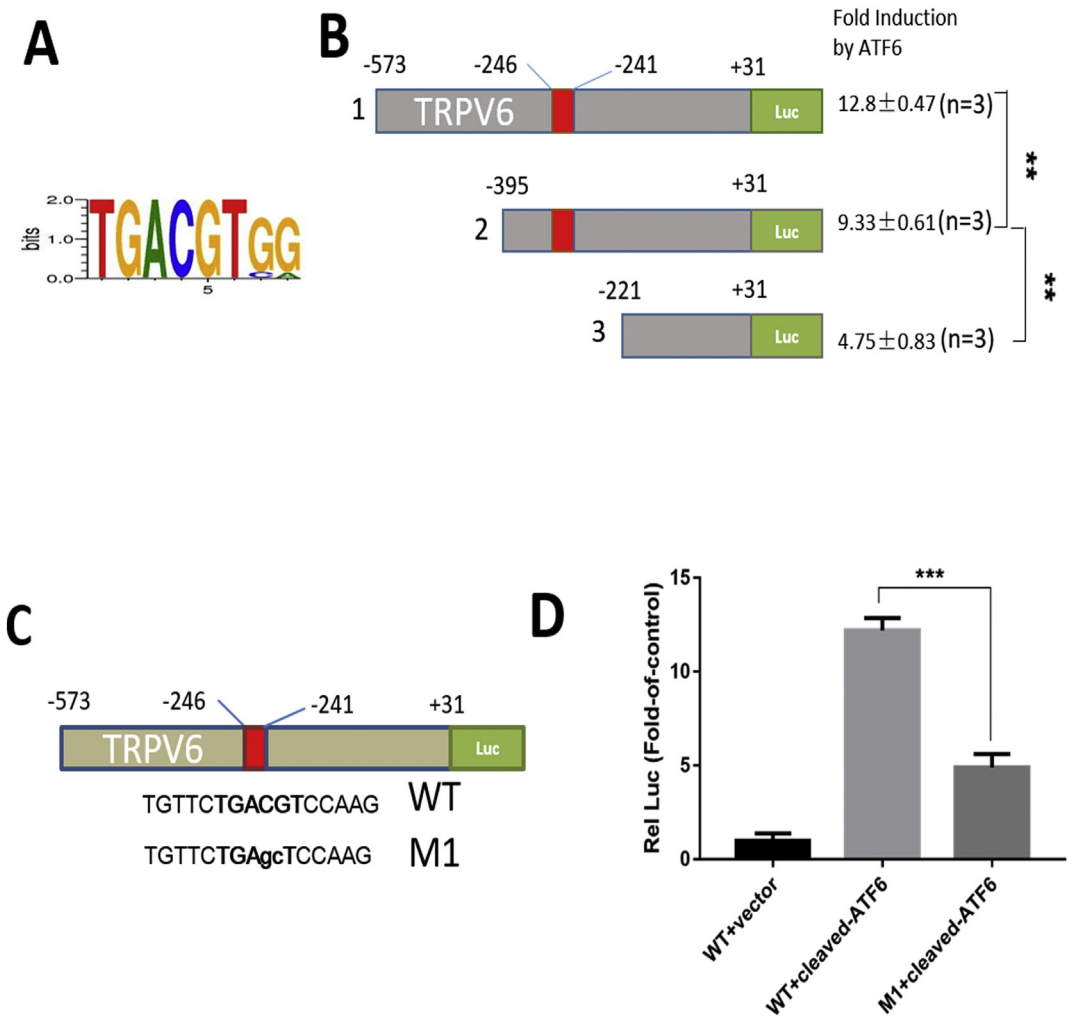

Fig. 4. Mutations at the putative ATF-6 binding site of TRPV6 promoter altered TRPV6 expression in hESC-CMs. A, the consensus binding motif for cleaved-ATF6 from http://motifmap.ics.uci.edu. B, human-TRPV6 (−573/+31)-Luc, human-TRPV6 (−395/+31)-Luc, and human-TRPV6 (−221/+31)-Luc were transfected into hESC-CMs. The cells were then infected with AAV-cleaved-ATF6α. Luciferase activity in each group was measured. C, illustration showing the nucleotide sequences of putative cleaved-ATF6 binding site (upper case) and its point mutant version (lower case) in the human TRPV6 promotor region. D, human-TRPV6 (−573/+31)-Luc (WT) and its point mutant version (M1) were transfected into hESC-CMs. The cells were then infected with AAV-vector or AAV-cleaved-ATF6α. Luciferase activity in each group was measured. Mean ± SEM (n = 3 independent experiments). $^{**}P < .01$, $^{***}P < .001$.

types. Reports showed that these TRP channels are situated upstream of the UPR in signaling cascade. The activity of these channels could either inhibit (TRPC1) or stimulate (TRPC3, −C6, −V1) the UPR [11–13]. However, in the present study, we found that knockdown of TRPV6 had no effect on the UPR, as determined by immunoblot analysis of GRP78 and CHOP, suggesting that TRPV6 was not situated upstream of the UPR. On the contrary, we found that TRPV6 was situated downstream of the UPR signaling cascade in hESC-CMs. Two lines of evidence suggest that, among the three signaling branches of UPR, the ATF6α branch was particularly important for the TRPV6 upregulation in hESC-CMs. 1) Based on immunoblot analysis of TRPV6 protein expression and dual luciferase assay of TRPV6 promoter, overexpression of cleaved ATF6α caused a marked increase in TRPV6 expression; 2) Point mutation at the putative ATF6 binding site on TRPV6 promoter substantially attenuated the stimulatory effect of cleaved ATF6α on TRPV6 expression. Taken together, these data demonstrate that TRPV6 is an ATF6-inducible gene under ER stress. We also found that ER stress could increase the expression of TRPC5 and TRPV5 proteins in hESC-CMs, which may be worth future exploration.

The UPR is initially an adaptive response to promote cell survival under ER stress. However, excessive or prolonged UPR owing to unresolved ER stress leads to apoptotic cell death. Thus, we next determined whether the upregulated TRPV6 expression under ER stress could promote cell survival or cause cell death. With the use of TUNEL assay and caspase-12 assay, we found that knockdown of TRPV6 stimulated apoptosis whereas overexpression of TRPV6 attenuated the apoptotic cell death, demonstrating a cytoprotective role of TRPV6 in the UPR in hESC-CMs. These results agree with the notion that ATF6-induced genes often contribute to adaptive ER stress responses but defends against maladaptive ER stress responses in cardiomyocytes [29].

Numerous studies reported that TRP channel-mediated Ca^{2+} influx may result in Ca^{2+} overload, leading to apoptotic cell death [12–15,30]. However, at least under certain circumstances, the activity of some TRP channels may promote cell survival and proliferation. For example, in LNCaP prostate cancer cells, TRPV6 mediates intracellular Ca^{2+} increase, promoting NFAT transcriptional factor-mediated signaling pathways, leading to an increased cell survival and resistance to apoptosis [17,18]. In addition, the activity of TRPC1 may promote the survival of mouse dopaminergic neurons under ER stress [11]. In the present study, we found that TRPV6 protects against ER stress-induced apoptotic cell death in hESC-CMs. However, unlike TRPC1, which is situated upstream of the UPR in signaling cascade [11], we found that TRPV6 is situated downstream of the UPR along its ATF6α axis.

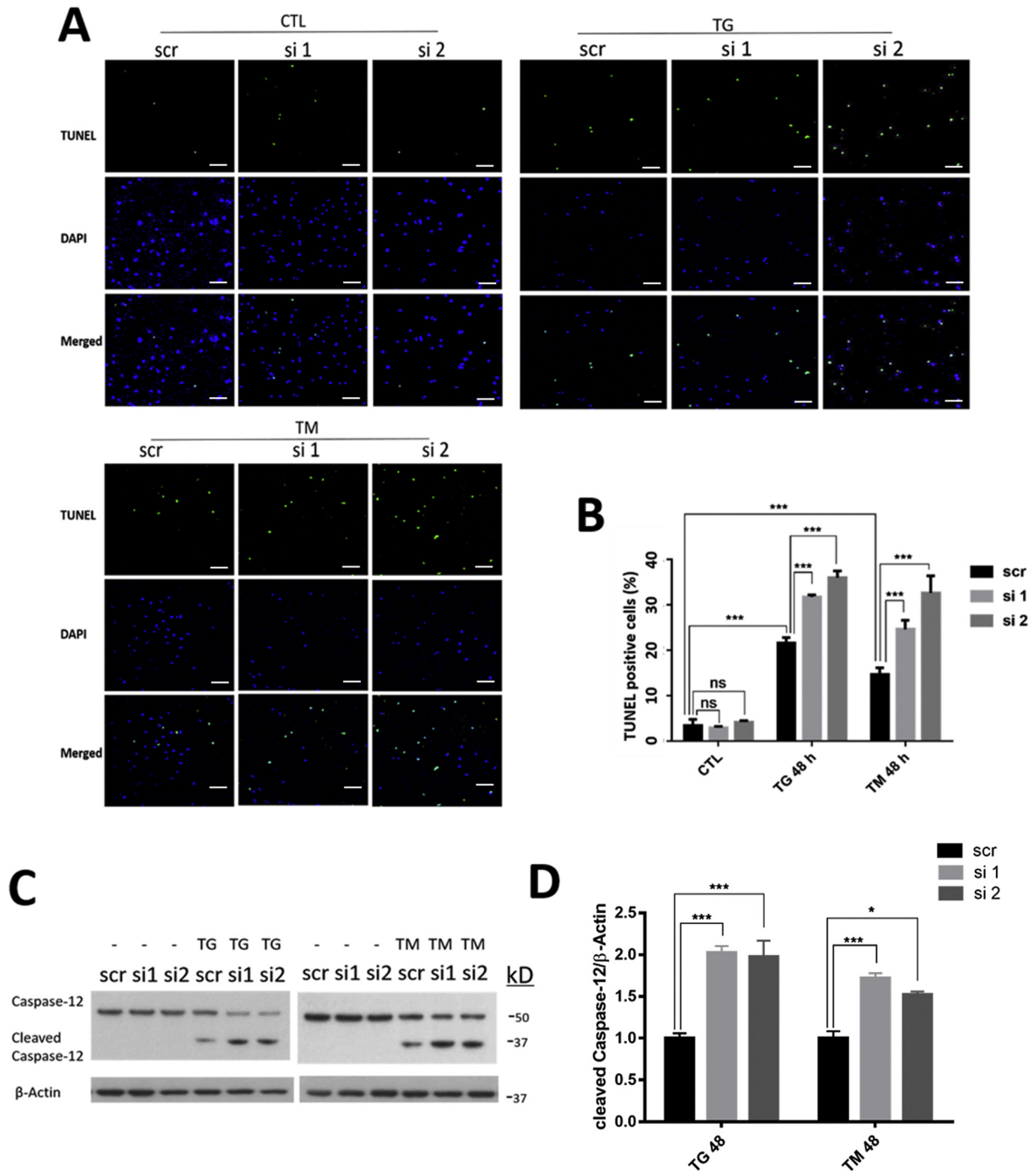

Fig. 5. Knockdown of TRPV6 increased ER stress-induced apoptosis. hESC-CMs were treated with lentivirus-based scrambled shRNA (scr), TRPV6-shRNA1 (si 1), or TRPV6-shRNA2 (si 2) for 72 h. The cells were then treated with vehicle (CTL), TG (100 nM), or TM (2 μg/ml) for 48 h. A and B, representative images (A) and summary data (B) showing TUNEL-positive apoptotic cells. The percentage of TUNEL positive cells was quantified. C and D, representative immunoblot images (C) and summary data (D) showing protein level of cleaved-caspase-12. Mean ± SEM (n = 3 independent experiments). *P < .05, **P < .01, ***P < .001, ns = not significant. Scale bar, 50 μm.

We next explored the signaling pathway downstream of TRPV6 that confers its cytoprotective effect in hESC-CMs. JNK is a key regulator of apoptosis [31]. ER stress can stimulate JNK to activate apoptotic pathway [27]. In the present study, knockdown of TRPV6 increased the JNK activity under prolonged ER stress whilst overexpression of TRPV6 attenuated the JNK activation. Moreover, in the presence of a JNK inhibitor SP600125, knockdown of TRPV6 could no longer increase the JNK activity or promote cell death under ER stress. These data suggested that TRPV6 may function to suppress JNK activity, resulting in its anti-apoptotic action. In addition, we also examined the possible role of TRPV6 in ERAD in hESC-CMs. However, knockdown of TRPV6 with TRPV6-siRNA had no effect on ERAD, suggesting that TRPV6 was not involved in ERAD under ER stress.

It is well documented that Ca^{2+} transients in cardiomyocytes are controlled by joint action of several Ca^{2+} handling proteins including L-type Ca^{2+} channels, type-2 ryanodine receptors, sarcoplasmic reticulum Ca^{2+}-ATPase and Na^{+}-Ca^{2+}-exchanger [32]. We explored whether TRPV6 could contribute to the Ca^{2+} transients in hESC-CMs.

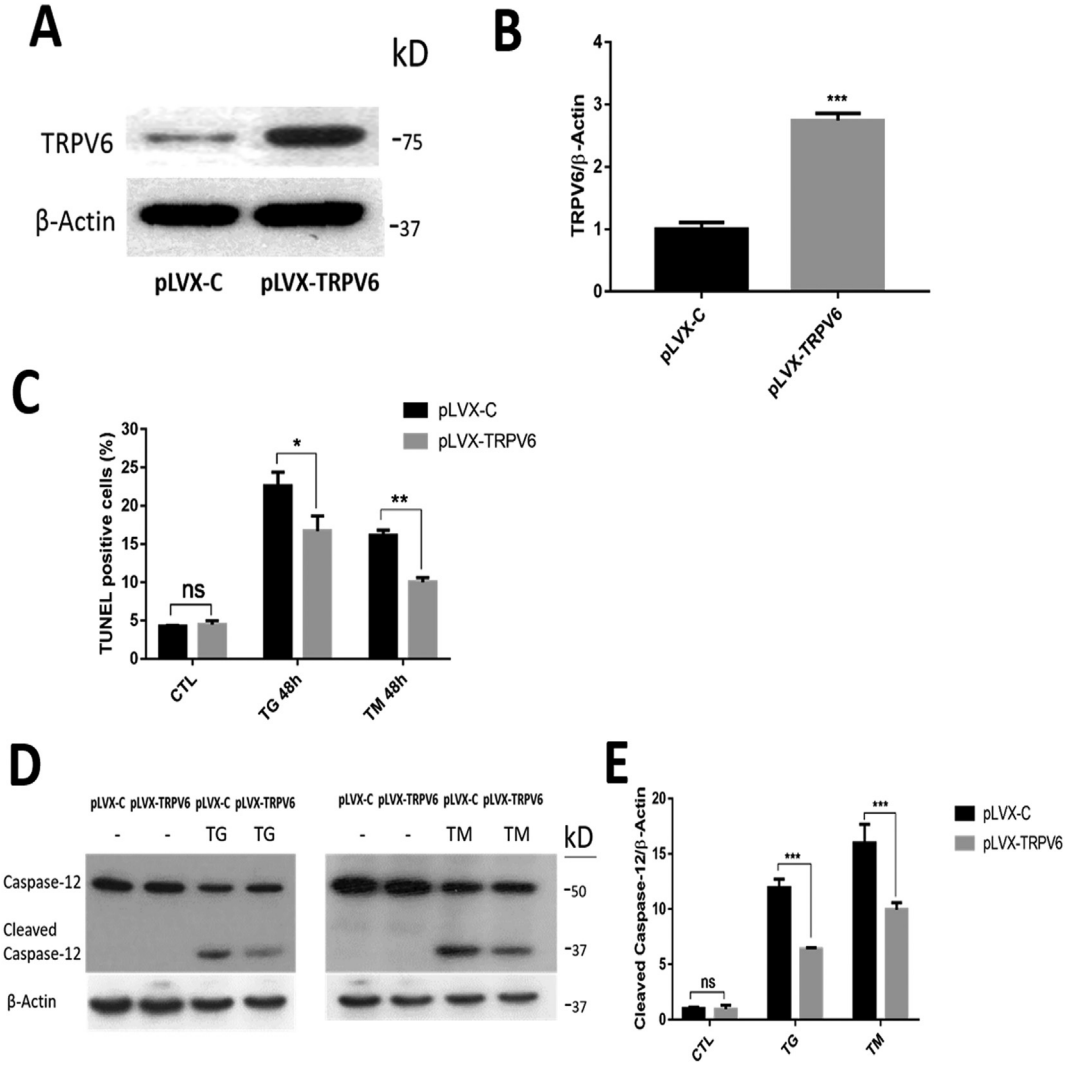

Fig. 6. Overexpression of TRPV6 reduced ER stress-induced apoptosis. hESC-CMs were treated with lentivirus-based empty vector (pLVX-C) or TRPV6 (pLVX-TRPV6) for 72 h. The cells were then treated with vehicle (CTL), TG (100 nM) or TM (2 μg/ml) for 48 h. A and B, representative immunoblot images (A) and summary data (B) showing the expressional level of TRPV6 proteins in pLVX-C group and pLVX-TRPV6 group. C, the percentage of TUNEL positive cells in each group. D and E, representative immunoblot images (D) and summary data (E) showing the protein level of cleaved-caspase-12 under different treatments. Mean ± SEM ($n = 3$ independent experiments). $^{*}P < .05$, $^{**}P < .01$, $^{***}P < .001$.

However, knockdown or overexpression of TRPV6 was found to have no effect on spontaneous and isoprenaline-stimulated cytosolic Ca^{2+} oscillations (Fig. S6). A likely explanation is that the TRPV6-mediated cytosolic Ca^{2+} change might be too small and/or local, which we could not detect in this study. On the other hand, we found that an ER stress inducer TG abolished the spontaneous and isoprenaline-stimulated cytosolic Ca^{2+} oscillations in hESC-CMs, which could not be restored by knockdown or overexpression of TRPV6 (Fig. S6). These data suggested that the ER stress inducer TG severely altered the Ca^{2+} homeostasis, which could not be restored by changing TRPV6 expression alone.

This study has some limitations. The cytoprotective role of TRPV6 against ER stress-induced cell death was only demonstrated with artificial ER stress inducers TG and TM. Although we have shown that TRPV6 is upregulated under physiological ER stress conditions, including ischemia-reperfusion in cultured hESC-CMs and myocardial infarction in vivo, the cytoprotective role of TRPV6 against ER stress-induced apoptosis has yet to be shown in these models. Further studies are needed to verify our hypothesis under these physiological ER stress conditions.

In conclusion, the present study demonstrates that ER stress causes an up-regulation of TRPV6 expression, which serves to protect hESC-CMs from ER stress-induced cell apoptosis. The signaling pathway involves ATF6α-TRPV6-JNK. The present study is the first report investigating ER stress and UPR in human pluripotent stem cell-derived cardiomyocytes. Our results thus provide valuable information for stem cell-based disease modeling and drug screening.

Acknowledgements

This work was supported by grants from Hong Kong Research Grant CommitteeAoE/M-05/12, TBRS/T13-706/11, 14118516, RGC-NSFC Joint Grant N_CUHK439/13, and China National Science Foundation Grant 31470912. We acknowledge Dr. Ron R. Kopito (Stanford University) for TCR-α-HA plasmid, and Dr. Natalia Prevarskaya (University of Lille) for pTRPV6-eYFP plasmid. GT is supported by the Croucher Foundation of Hong Kong.

Conflicts of interest

The authors declare that none of them have any conflict of interest.

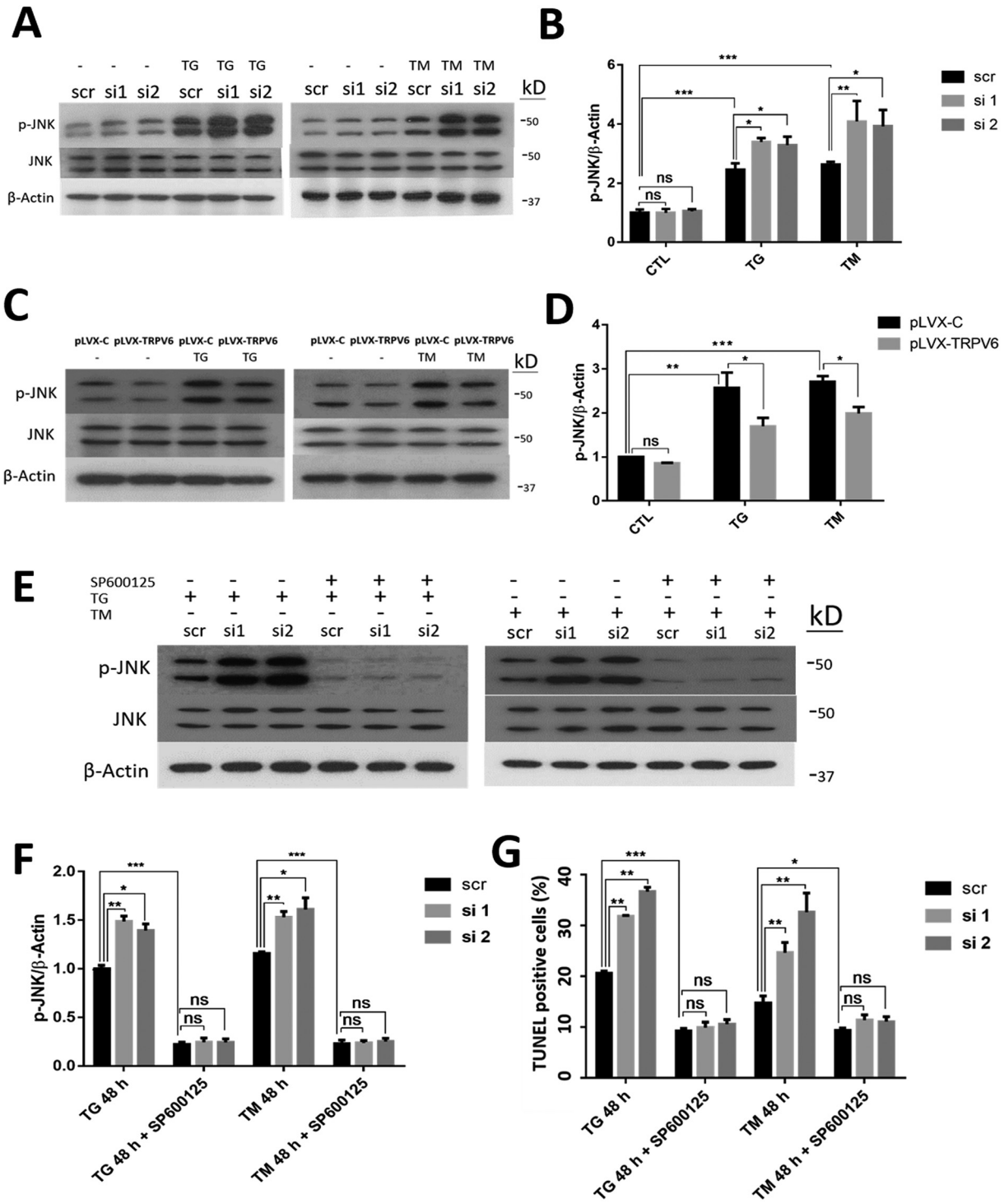

Fig. 7. JNK signaling pathway was downstream of TRPV6. A and B, hESC-CMs were treated with lentivirus-based scrambled shRNA (scr), TRPV6-shRNA1 (si 1), or TRPV6-shRNA2 (si 2) for 72 h. The cells were then treated with vehicle (CTL), TG (100 nM), or TM (2 μg/ml) for 48 h. C and D, hESC-CMs were treated with lentivirus-based empty vector (pLVX-C) or TRPV6 (pLVX-TRPV6) for 72 h. The cells were then treated with vehicle, TG (100 nM), or TM (2 μg/ml) for 48 h. E - G, hESC-CMs were treated with lentivirus-based scrambled shRNA (scr), TRPV6-shRNA1 (si 1), or TRPV6-shRNA2 (si 2) for 72 h. The cells were then treated with TG (100 nM) or TM (2 μg/ml) in the absence or presence of SP600125 (20 μM) for 48 h. Shown are representative immunoblot images (A, C, E) and summary data (B, D, F) of p-JNK and JNK protein levels. G shows the percentage of TUNEL positive cells. Mean ± SEM (n = 3 independent experiments). *P < .05, **P < .01, ***P < .001, ns = not significant.

Appendix A. Supplementary data

Supplementary data to this article can be found online at https://doi.org/10.1016/j.yjmcc.2018.05.008.

References

[1] M. Wang, R.J. Kaufman, The impact of the endoplasmic reticulum protein-folding environment on cancer development, Nat. Rev. Cancer 14 (2014) 581–597.
[2] K.R. Boheler, J. Czyz, D. Tweedie, H.T. Yang, S.V. Anisimov, A.M. Wobus, Differentiation of pluripotent embryonic stem cells into cardiomyocytes, Circ. Res.

91 (2002) 189–201.
[3] G. Földes, M. Mioulane, J.S. Wright, A.Q. Liu, P. Novak, B. Merkely, et al., Modulation of human embryonic stem cell-derived cardiomyocyte growth: a testbed for studying human cardiac hypertrophy? J. Mol. Cell. Cardiol. 50 (2011) 367–376.
[4] H. Hamada, M. Suzuki, S. Yuasa, N. Mimura, N. Shinozuka, Y. Takada, et al., Dilated cardiomyopathy caused by aberrant endoplasmic reticulum quality control in mutant KDEL receptor transgenic mice, Mol. Cell. Biol. 24 (2004) 8007–8017.
[5] A. Brodarac, T. Šarić, B. Oberwallner, S. Mahmoodzadeh, K. Neef, J. Albrecht, et al., Susceptibility of murine induced pluripotent stem cell-derived cardiomyocytes to hypoxia and nutrient deprivation, Stem Cell Res Ther 6 (2015) 1–19.
[6] G. Gao, A. Xie, J. Zhang, A.M. Herman, E.M. Jeong, L. Gu, et al., Unfolded protein response regulates cardiac sodium current in systolic human heart failure, Circ. Arrhythm. Electrophysiol. 6 (2013) 1018–1024.
[7] J.M. Nerbonne, Studying cardiac arrhythmias in the mouse—a reasonable model for probing mechanisms? Trends Cardiovasc. Med. 14 (2004) 83–93.
[8] I. Kehat, D. Kenyagin-Karsenti, M. Snir, H. Segev, M. Amit, A. Gepstein, et al., Human embryonic stem cells can differentiate into myocytes with structural and functional properties of cardiomyocytes, J. Clin. Invest. 108 (2001) 407–414.
[9] J. Liu, Z. Zhang, Y. Liu, C. Guo, Y. Gong, S. Yang, et al., Generation, characterization, and potential therapeutic applications of cardiomyocytes from various stem cells, Stem Cells Dev. 21 (2012) 2095–2110.
[10] J. Zheng, Molecular mechanism of TRP channels, Compr. Physiol. 3 (2013) 221–242.
[11] S. Selvaraj, Y. Sun, J.A. Watt, S. Wang, S. Lei, L. Birnbaumer, et al., Neurotoxin-induced ER stress in mouse dopaminergic neurons involves downregulation of TRPC1 and inhibition of AKT/mTOR signaling, J. Clin. Invest. 122 (2012) 1354–1367.
[12] P.T. Ampem, K. Smedlund, G. Vazquez, Pharmacological evidence for a role of the transient receptor potential canonical 3 (TRPC3) channel in endoplasmic reticulum stress-induced apoptosis of human coronary artery endothelial cells, Vasc. Pharmacol. 76 (2016) 42–52.
[13] K.C. Thomas, A.S. Sabnis, M.E. Johansen, D.L. Lanza, P.J. Moos, G.S. Yost, et al., Transient receptor potential vanilloid 1 agonists cause endoplasmic reticulum stress and cell death in human lung cells, J. Pharmacol. Exp. Ther. 321 (2007) 830–838.
[14] K.C. Thomas, J.K. Roberts, C.E. Deering-Rice, E.G. Romero, R.O. Dull, J. Lee, et al., Contributions of TRPV1, endovanilloids, and endoplasmic reticulum stress in lung cell death in vitro and lung injury, Am. J. Phys. Lung Cell. Mol. Phys. 302 (2012) L111–L119.
[15] S. Chen, F.F. He, H. Wang, Z. Fang, N. Shao, X.J. Tian, et al., Calcium entry via TRPC6 mediates albumin overload-induced endoplasmic reticulum stress and apoptosis in podocytes, Cell Calcium 50 (2011) 523–529.
[16] C. Fecher-Trost, P. Weissgerber, U. Wissenbach, TRPV6 channels, Handb. Exp. Pharmacol. 222 (2014) 359–384.
[17] M. Raphaël, V. Lehen'kyi, M. Vandenberghe, B. Beck, S. Khalimonchyk, F. Vanden Abeele, et al., TRPV6 calcium channel translocates to the plasma membrane via Orai1-mediated mechanism and controls cancer cell survival, Proc. Natl. Acad. Sci. U. S. A. 111 (2014) E3870–E3879.
[18] V. Lehen'kyi, M. Flourakis, R. Skryma, N. Prevarskaya, TRPV6 channel controls prostate cancer cell proliferation via Ca^{2+}/NFAT-dependent pathways, Oncogene 26 (2007) 7380–7385.
[19] J.K. Lau, K.C. Brown, A.M. Dom, T.R. Witte, B.A. Thornhill, C.M. Crabtree, et al., Capsaicin induces apoptosis in human small cell lung cancer via the TRPV6 receptor and the calpain pathway, Apoptosis 19 (2014) 1190–1201.
[20] J. Chow, M. Norng, J. Zhang, J. Chai, TRPV6 mediates capsaicin-induced apoptosis in gastric cancer cells–mechanisms behind a possible new "hot" cancer treatment, Biochim. Biophys. Acta 1773 (2007) 565–576.
[21] Z. Weng, C.W. Kong, L. Ren, I. Karakikes, L. Geng, J. He, et al., A simple, cost-effective but highly efficient system for deriving ventricular cardiomyocytes from human pluripotent stem cells, Stem Cells Dev. 23 (2014) 1704–1716.
[22] L. Wang, J.Y. Luo, B. Li, X.Y. Tian, L.J. Chen, Y. Huang, et al., Integrin-YAP/TAZ-JNK cascade mediates atheroprotective effect of unidirectional shear flow, Nature 540 (2016) 579–582.
[23] H. Yu, G. Kaung, S. Kobayashi, R.R. Kopito, Cytosolic degradation of T-cell receptor alpha chains by the proteasome, J. Biol. Chem. 272 (1997) 20800–20804.
[24] Y. Wang, Z.C. Li, P. Zhang, E. Poon, C.W. Kong, K.R. Boheler, et al., Nitric oxide-cGMP-PKG pathway acts on Orai1 to inhibit the hypertrophy of human embryonic stem cell-derived cardiomyocytes, Stem Cells 33 (2015) 2973–2984.
[25] T. Nakagawa, H. Zhu, N. Morishima, E. Li, J. Xu, B.A. Yankner, et al., Caspase-12 mediates endoplasmic-reticulum-specific apoptosis and cytotoxicity by amyloid-beta, Nature 403 (2000) 98–103.
[26] S. Elmore, Apoptosis: a review of programmed cell death, Toxicol. Pathol. 35 (2007) 495–516.
[27] R. Iurlaro, C. Muñoz-Pinedo, Cell death induced by endoplasmic reticulum stress, FEBS J. 283 (2016) 2640–2652.
[28] S. Doroudgar, M. Völkers, D.J. Thuerauf, M. Khan, S. Mohsin, J.L. Respress, et al., Hrd1 and ER-associated protein degradation, ERAD, are critical elements of the adaptive ER stress response in cardiac myocytes, Circ. Res. 117 (2015) 536–546.
[29] C.C. Glembotski, Roles for ATF6 and the sarco/endoplasmic reticulum protein quality control system in the heart, J. Mol. Cell. Cardiol. 71 (2014) 11–15.
[30] I. Fliniaux, E. Germain, V. Farfariello, N. Prevarskaya, TRPs and Ca2+ in cell death and survival, Cell Calcium 69 (2018) 4–18.
[31] J. Liu, A. Lin, Role of JNK activation in apoptosis: a double-edged sword, Cell Res. 15 (2005) 36–42.
[32] D.M. Bers, Cardiac excitation-contraction coupling, Nature 415 (2002) 198–205.